euronoise 2021
25th to 27th of October
Madeira, Portugal - online

Sound diffusing metasurfaces based on elastic plates and membranes

José M. Requena-Plens[1], Jean-Philippe Groby[2], Vicent Romero-García[2], Noé Jiménez[1,*]

[1] Instituto de Instrumentación para Imagen Molecular, Universitat Politècnica de València - CSIC, València, Spain
* nojigon@upv.es
[2] Laboratoire d'Acoustique de l'Université du Mans (LAUM), UMR 6613,
Institut d'Acoustique - Graduate School (IA-GS), CNRS, Le Mans Université, Le Mans, France

Abstract
Traditional acoustic diffusers are based on quarter-wavelength resonators, and they are commonly built using slotted panels. The use of this kind of resonators implies that these panels can hardly be manufactured to work at low frequencies due to the resulting high thickness. Recently, the use of resonant metamaterials based on Helmholtz resonators, i.e., metadiffusers, has been proposed to reduce panel thickness. In this work we propose the use of plate and membrane (I will use only plate) resonators to go one step further in managing sound reflection using ultrathin metasurfaces of deep subwavelength dimensions. Using a 5.7-cm thick panel, a mean diffusion coefficient of 0.8 in the range from 400 to 800 Hz has been numerically and theoretically observed. The potential of resonant metamaterials based on plate and membrane resonators is demonstrated and its limitations discussed. This study provides the guidelines and design tools for prototyping these low-thicknesses panels to generate diffuse reflections.

Keywords: sound diffusers, metamaterials, metasurfaces, scattering, elastic plates.

1 Introduction

Nowadays, research on acoustic metasurfaces is very active. However, the use of locally resonant structures to control sound diffusion in room acoustics dates to the late 70's, when arrangements of quarter-wavelength resonators, called phase-grating diffusers, were introduced by M. Schröeder to generate diffuse reflections [1]. These acoustic devices have found practical applications in room acoustics and are widely used in many broadcast studios, modern auditoria, music recording, control, and rehearsal rooms [2]. Recently, metamaterials were proposed to reduce the thickness of Schröeder diffusers by using Helmholtz resonators instead of quarter-wavelength resonators [3] or slow-sound metasurfaces with deep-subwavelength resonators [4], [5]. Recently, the scattering properties of spiral metasurfaces based on holographic acoustic vortices was presented [6], by making use of vorticity it was possible to design broadband and non-specular sound diffusing surfaces. Other strategy is to use membranes or plates instead of quarter-wavelength resonators or Helmholtz resonators. In a plate, or a membrane, the resonance in the plate arises due to the transversally propagating waves in the elastic solid. Therefore, the resonance can be tuned by several mechanisms. First, it can be tuned by modifying the elastic parameters of the elastic solid (in the case of plates) or the tension (in the case of the membranes). However, this process can be cumbersome for practical reasons. Other approach is to modify the mass density of a membrane by adding a localized mass [7], but,

again, the fine required tuning becomes difficult in a practical implementation. In this work, we propose to use a panel composed of a square array of resonating thin plates, each one backed by a cavity, as shown in Fig. 1. By tuning the depth of the backing cavity, it is possible to tune the resonance frequency of each cell using the same plate. In this way, we can engineer the metasurface in a robust way, resulting in thin and easy-to-build sound diffusers.

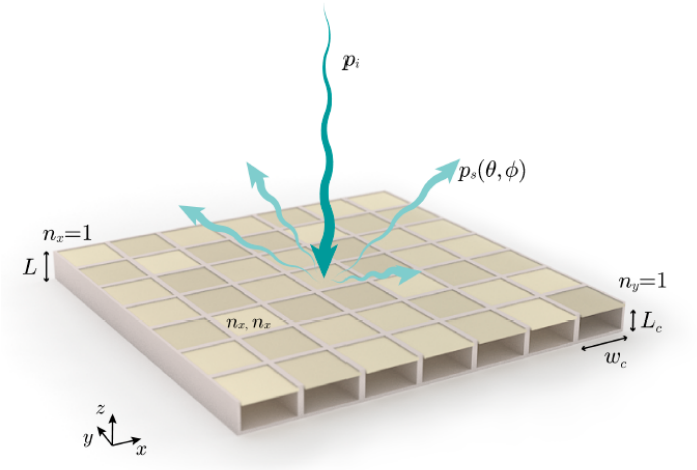

Figure 1 –Scheme of a sound diffuser based on elastic plates.

2 Methods

We model the unit cell as a clamped rectangular elastic plate backed by a cavity, as shown in Fig. 1. We follow the model presented by Sun and Jan [8]. For a square clamped plate of side a, the orthogonal modal decomposition of the displacement components of the plate given by, $X_m(x)$, $Y_n(y)$ gives

$$\begin{aligned} X_m(x) &= G\left(\frac{\lambda_m x}{a}\right) - \frac{G(\lambda_m)}{H(\lambda_m)} H\left(\frac{\lambda_m x}{a}\right), \\ Y_n(y) &= G\left(\frac{\lambda_n y}{a}\right) - \frac{G(\lambda_n)}{H(\lambda_n)} H\left(\frac{\lambda_n y}{a}\right), \end{aligned} \tag{1}$$

with the functions $G(u)$ and $H(u)$ given by

$$\begin{aligned} G(u) &= \cosh(u) - \cos(u), \\ H(u) &= \sinh(u) - \sin(u), \end{aligned} \tag{2}$$

and where λ_m and λ_n satisfy

$$\cosh(\lambda)\cos(\lambda) = 1, \tag{3}$$

that can be solved numerically, e.g., by using Muller's method [9]. Then, we can define the following integrals

$$
\begin{aligned}
I_1 &= \int_0^a X_m(x)\frac{\partial^4 X_m(x)}{\partial x^4}dx, \qquad I_2 &= \int_0^a Y_n^2 dy, \\
I_3 &= \int_0^a X_m(x)\frac{\partial^2 X_m(y)}{\partial x^2}dx, \qquad I_4 &= \int_0^a Y_n(y)\frac{\partial^2 Y_n(y)}{\partial x^2}dy, \\
I_5 &= \int_0^a Y_n(y)\frac{\partial^4 Y_n(y)}{\partial x^4}dy, \qquad I_6 &= \int_0^a X_m(x)^2 dx.
\end{aligned} \tag{4}
$$

These integrals can be numerically integrated using the Simpson's rule. Finally, the impedance of the plate is defined as

$$
Z_p(\omega) = \left[i\omega \iint_0^a \left(\sum_{m=1}^{\infty}\sum_{n=1}^{\infty} \frac{\iint_0^a X_m Y_n dxdy}{D(I_1 I_2 + 2I_3 I_4 + I_5 I_6) - \rho h \omega^2 I_2 I_6} \right) dxdy \right]^{-1}. \tag{5}
$$

where ρ is the density, and h is the thickness of the plate, and its bending stiffness (or flexural rigidity), D, is given by

$$
D = \frac{Eh^3}{12(1-\nu^2)}, \tag{6}
$$

the wavenumber in the plate follows the dispersion relation

$$
k^2 = \omega\sqrt{\frac{\rho h}{D}}, \tag{7}
$$

and E and ν, the Young's modulus and Poisson's ratio of the material plate, respectively. The resonance frequencies of the plate without the backing are given by

$$
\omega_{m,n} = \sqrt{\frac{D(I_1 I_2 + 2I_3 I_4 + I_5 I_6)}{\rho h I_2 I_6}}. \tag{8}
$$

It is worth to mention that a low-frequency approximation of the elastic plate can be obtained using a lumped model. The effective mass and compliance of the plate for the first resonance mode are given by

$$
C_p = 3.73 ¥ 10^{-4}\frac{a^6}{D}, \qquad M_p = 2.06\frac{r}{a^2}, \tag{9}
$$

And the impedance of the lumped plate is

$$
Z_{lumped} = \frac{1}{iwC_p} + iwM_p, \tag{10}
$$

In this case the resonance frequency is given by $\mathrm{Im}(Z_p) = 0$, so the frequency is $w_0 = \sqrt{1/M_p C_p}$. Finally, the total impedance at the surface of each cell is given by

$$
Z_T = Z_p + iZ_0 \cot(kL), \tag{11}
$$

where L is the depth of the cavity and $Z_0 = \rho_0 c_0 / a^2$ is the impedance normalized by the surface, ρ_0 the density and c_0 the sound speed of the air. The impedance of the plate can by set to the full model given by

Eq. (5) or the lumped model (10). In this case, the resonance frequency can be downshifted deeper in the subwavelength regime. Using this impedance, the reflection coefficient for each cell, located at in the plane x_0, y_0 and at $z = 0$, can be calculated as

$$R(x,y) = \frac{Z_T(x_0,y_0) - Z_0}{Z_T(x_0,y_0) + Z_0}. \tag{12}$$

Then, the acoustic field at a point $\mathbf{r} = \mathbf{r}(x,y,z)$ scattered by the metasurface located at $\mathbf{r}_0 = \mathbf{r}_0(x,y,z=0)$ can be approximated by the Rayleigh-Sommerfeld integral as

$$p_s(\mathbf{r}) = -i\frac{k}{2\pi}\int_{S_0} \frac{p_0(\mathbf{r_0})R(\mathbf{r_0})\exp(ik|\mathbf{r}-\mathbf{r}_0|)}{|\mathbf{r}-\mathbf{r}_0|} dS_0, \tag{13}$$

where $p_0(\mathbf{r}_0)$ is the incident pressure field, $R(\mathbf{r}_0)$ is the spatially-dependent reflection coefficient of the locally-reacting surface, given by (12), over the surface S_0, and $k = \omega / c_0$ is the wavenumber in air at an angular frequency ω, and c_0 is the sound speed. In the far field, and in spherical coordinates, $\mathbf{r} = \mathbf{r}(\phi,\theta,r)$, using the convention $0 < \phi < 2\pi$ for the azimuth and $0 < \theta < \pi$ for the elevation, the distance between any point and the plane of the metasurface is approximated by

$$|\mathbf{r}-\mathbf{r}_0| \approx r. \tag{14}$$

A second-order Taylor expansion yields

$$|\mathbf{r}-\mathbf{r}_0| \approx r - \frac{x}{r}x_0 - \frac{y}{r}y_0 \approx r - \cos\phi\sin\theta x_0 - \sin\phi\sin\theta y_0. \tag{15}$$

Introducing the approximation given by (14) in the denominator of (13) and the expansion (15) in the exponential of the numerator of (13), respectively, we get the Fraunhofer-Fourier approximation of the scattered field as

$$p_s(\phi,\theta) = -i\frac{k}{2\pi}\frac{\exp(ikr)}{r}\int_{S_0} p_0(x_0,y_0)R(x_0,y_0)\exp(-i(k_x x_0 + k_y y_0))dx_0 dy_0, \tag{16}$$

where the transversal components of the wavevector are given by

$$k_x = k\cos\phi\sin\theta, \quad \text{and} \quad k_y = k\sin\phi\sin\theta. \tag{17}$$

Note the spherical-divergence factor $\exp(ikr)/r$ is usually dropped as it does not contribute to the directivity of the scattering in the azimuthal and elevation planes. Equation (16) is essentially a two-dimensional spatial Fourier transform of the reflected field and can be calculated efficiently using fast-Fourier transforms. In this work, we tune the complex reflection coefficient $R(x_0,y_0)$ along the surface of the structure using elastic plates to produce far-field scattering $p_s(\phi,\theta)$ with is uniform with the azimuthal and elevation angles.

3 Results

3.1 The impedance of a rigidly-backed elastic plate

We start by revisiting the impedance of an elastic plate backed by a cavity. We are interested in thin panels, so the quarter wavelength resonance frequency of the cavity is much higher than the resonance of the plate. In this regime, the cavity has a great impact on the resonance of the unit cell. The resonance modes are

observed at frequencies when the system does not present any reacting behaviors and the imaginary part of the impedance is null. Figure 2 (left) shows the imaginary part of the impedance. First, the lumped model (blue curve) shows that the imaginary part vanishes at one single point. The cavity alone is shown in black. It crosses the cero at much higher frequency, 2000 Hz, corresponding this frequency with its quarter wavelength resonance. However, we can see that the imaginary part of the cavity, given by the cotangent function, presents two limiting values. In the low frequency limit, the imaginary part of the impedance of the cavity presents a very large value, so when combining this impedance in series with the plate, the cavity dominates. In this regime, the whole unit cell cannot present any resonance and, therefore, acts as a rigid wall. At medium frequencies, we can see that the cavity shifts the resonance of the plate to a higher frequency.

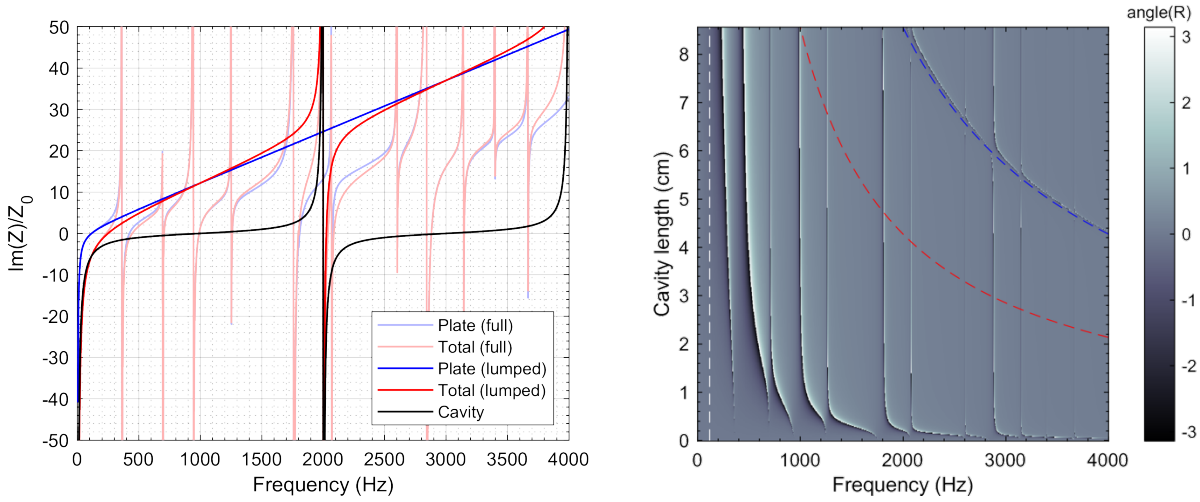

Figure 2. Imaginary part of the impedance of a plate backed by a cavity of 8.55 cm. (right) Phase of the reflection coefficient of the unit cell as a function of the length of the cavity and the frequency. The quarter wavelength resonance of the cavity is shown in dashed red, and its antiresonance frequency is shown in dashed blue.

At this point, is convenient to include in the analysis the full model, as the validity of the lumped model is restricted for frequencies up to the first resonance. We might note that the full model includes both, resonances, at the zero-crossings in Fig. 2, (left), and antiresonances, shown as discontinuities in Fig. 2 (left). Therefore, when combining in series a plate with a cavity, the resonance frequency cannot be shifted beyond the antiresonance because the latter introduces a discontinuity on the imaginary part of the impedance and the total impedance around this frequency range is dominated by the antiresonance. This effect is revealed to be critical when designing metasurfaces based on elastic plates and membranes, as we will see below. Taking the full model into account, we can observe that other modes are present, corresponding each one to the normal modes of the elastic vibrating plate. Finally, in the high frequency regime, the imaginary part of the impedance of the cavity starts to diverge, because of its antiresonance. This corresponds to the half-wavelength resonance of the cavity. Here, the cavity acts as a rigid element. In this regime, the cavity dominates the total impedance, the summation of both elements results in a shifting of the plate resonances to lower frequencies, but this shift is restricted to their nearest antiresonance. This process results in narrowband resonances at high frequency. In summary, while the resonance of the plate can be tuned in

some degree just using a rigidly-backed cavity, at the antiresonance frequencies the whole unit cell acts as a reflecting panel, and these frequencies remain fixed by the plate (or a membrane).

The phase of the reflection coefficient as a function of the length of the cavity is shown in Fig. 2 (right). We can see that at the resonance of the unit cell, a phase jump is produced, $\arg(R) = \pm p$. Using a sub-wavelength depth cavity, the first resonance frequency is shifted at frequencies higher than the resonance of the plate (dashed white). Therefore, the first and the superior resonances can be tuned by the length of the cavity. We might notice that there are frequency ranges where no resonance is present. This is caused by the antiresonances of the plate. At these frequencies, the whole unit cell acts as a rigid boundary and other mechanism must be included to tune the reflection coefficient at these frequencies. These include changing the material of the membrane, its thickness, its surface or adding mass.

3.2 Tuning the reflection coefficient

Using the degree of freedom of the backing cavity, we can tune the reflection coefficient. For example, que can tune the reflection coefficient of a plate-metadiffuser of maximum thickness of L = 2 cm, to that of a quadratic residue diffuser of L = 16 cm, both designed to work at 1200 Hz. The resulting phase is shown in Fig. 3, where it can be observed a good agreement between both distributions. As the reflection coefficient along the surface is the same in both cases, it is not surprising that the far field scattering, shown in Fig.4 is similar. If compared with a flat reflector, we can see that both structures scatter waves in multiple directions, following a similar and uniform pattern. Therefore, both structures present a similar normalized diffusion coefficient, 0.67 for the QRD and 0.69 for the plate metadiffuser. The main difference is that the thickness of the metadiffuser is about 10 times thinner.

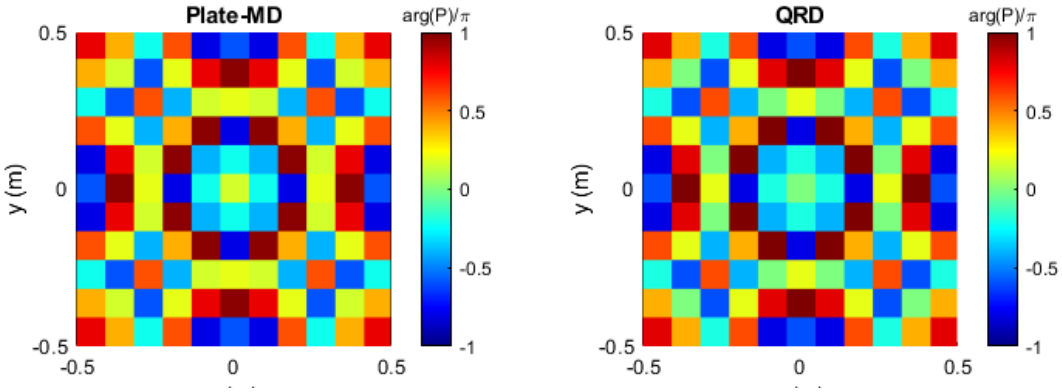

Figure 3 – (left) phase of the reflection coefficient for a plate-metadiffuser of L= 2 cm, at 1200 Hz, tuned to be the same than the phase of a quadratic residue diffusers of L = 16 cm, designed for the same frequency.

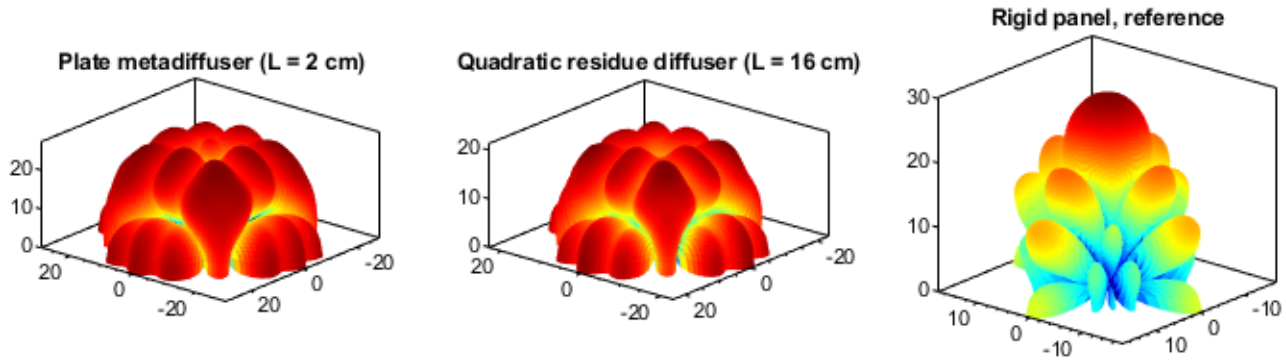

Figure 4 – (left) Resulting far-field scattering of the plate-metadiffuser, (center) QRD, and (right) rigid panel.

4 Conclusions

Using plate resonators panels with broadband response can be optimized. However, as the bandwidth of the resonance is narrow, the diffusion coefficient should present a band-limited response. Other drawback is that, using plates, the absorption coefficient cannot be tuned as easily as using Helmholtz resonators. In addition, practical implementation of membrane and plate resonators usually differs from modelling. We expect that this effect will result in a performance decrease of optimized panels in realistic situations. However, other topologies can be explored to mitigate these factors. For example, by locating the plates at the middle of the cavity the high-frequency response can be enhanced. On the other hand, using several thicknesses for the plates will eliminate the rigid behaviour of the panel at the antiresonances. This works opens new paths to design shallow panels to control the scattering of acoustic waves where space is limited, such as designing sound diffusers for critical listening rooms, or designing thin diffusing metasurfaces for underwater applications.

Acknowledgements

We acknowledge financial support from the Spanish Ministry of Science, Innovation and Universities through grant “Juan de la Cierva – Incorporación” (IJC2018-037897-I) and PID2019-111436RB-C22, and by the Agència Valenciana de la Innovació through grants INNVAL10/19/016. This article is based upon work from COST Action DENORMS CA15125. JPG and VRG gratefully acknowledge projects ANR-RGC METARoom (ANR-18-CE08-0021) and the HYPERMETA funded under the program Étoiles Montantes of the Région Pays de la Loire.

References

[1] M. R. Schroeder, “Diffuse sound reflection by maximum−length sequences,” *J. Acoust. Soc. Am.*, vol. 57, no. 1, pp. 149–150, Jan. 1975, doi: 10.1121/1.380425.

[2] T. J. Cox and P. D’Antonio, *Acoustic Absorbers and Diffusers*. Crc Press, 2009.

[3] Y. Zhu, X. Fan, B. Liang, J. Cheng, and Y. Jing, “Ultrathin acoustic metasurface-based schroeder diffuser,” *Phys. Rev. X*, vol. 7, no. 2, p. 21034, 2017, doi: 10.1103/PhysRevX.7.021034.

[4] N. Jiménez, T. J. Cox, V. Romero-García, and J. P. Groby, “Metadiffusers: Deep-subwavelength

sound diffusers," *Sci. Rep.*, 2017, doi: 10.1038/s41598-017-05710-5.

[5] E. Ballestero, N. Jiménez, J. P. Groby, S. Dance, H. Aygun, and V. Romero-García, "Experimental validation of deep-subwavelength diffusion by acoustic metadiffusers," *Appl. Phys. Lett.*, vol. 115, no. 8, p. 081901, Aug. 2019, doi: 10.1063/1.5114877.

[6] N. Jiménez, J. P. Groby, and V. Romero-García, "Spiral sound-diffusing metasurfaces based on holographic vortices," *Sci. Rep.*, vol. 11, no. 1, 2021, doi: 10.1038/s41598-021-89487-8.

[7] Y.-T. Wang and R. Craster, "Designing Hyper-Thin Acoustic Metasurfaces with Membrane Resonators."

[8] C. C. Sung and J. T. Jan, "The response of and sound power radiated by a clamped rectangular plate," *J. Sound Vib.*, 1997, doi: 10.1006/jsvi.1997.1125.

[9] D. E. Muller, "A Method for Solving Algebraic Equations Using an Automatic Computer," *Math. Tables Other Aids to Comput.*, vol. 10, no. 56, p. 208, 1956, doi: 10.2307/2001916.